

# Optimization of Antireflective Layers of Silicon Solar Cells: Comparative Studies of the Efficiency Between Single and Double Layer at the Reference Wavelength

**Alassane Diaw<sup>\*</sup>, Awa Dieye, Ousmane Ngom, Moulaye Diagne, Nacire Mbengue, Oumar Absatou Niasse, Bassirou Ba**

Laboratory of the Semiconductors and Solar Energy (LASES), Department of Physics, Faculty of Sciences and Techniques, University Cheikh Anta Diop, Dakar, Senegal

## Email address:

[alou2045@yahoo.fr](mailto:alou2045@yahoo.fr) (A. Diaw)

<sup>\*</sup>Corresponding author

## To cite this article:

Alassane Diaw, Awa Dieye, Ousmane Ngom, Moulaye Diagne, Nacire Mbengue, Oumar Absatou Niasse, Bassirou Ba. Optimization of Antireflective Layers of Silicon Solar Cells: Comparative Studies of the Efficiency Between Single and Double Layer at the Reference Wavelength. *American Journal of Physics and Applications*. Vol. 9, No. 6, 2021, pp. 133-138. doi: 10.11648/j.ajpa.20210906.11

**Received:** August 31, 2021; **Accepted:** September 22, 2021; **Published:** November 5, 2021

---

**Abstract:** The deposition of an antireflection coating (ARC) on the front side of the solar cells allows a significant reduction of the losses by reflection. It thus allows an increase in the efficiency of the cells. Various materials are used as an antireflection layer. For our studies, we focused on the deposition of some materials as an antireflection layer on the solar cell such as SiO<sub>2</sub>, Si<sub>3</sub>N<sub>4</sub>, TiO<sub>2</sub>, Al<sub>2</sub>O<sub>3</sub>, MgF<sub>2</sub>, and studied the efficiency of the latter. A theoretical study of antireflection layers has shown that a single antireflection layer does not have as low a reflectivity as a double antireflection layer over a large wavelength range. Thus, our interest was focused on double and multiple antireflection layers. The influence of parameters such as the thickness of the layer (s) as well as the associated refractive indexes on the optical properties of the antireflective structure has been studied. It was found that there are optimal thicknesses and refractive indices for which the reflectivity of the antireflective system is almost zero over a wider or shorter range of wavelengths. The same phenomena are noted in the study of the external quantum efficiency of the solar cell with these materials.

**Keywords:** Silicon, Antireflective Coatings, Solar Cell, Reflection, Transmission, External Quantum Efficiency

---

## 1. Introduction

The application of anti-reflective layers is one of the most effective ways to improve the performance of solar cells. The antireflection coating (ARC) is able to effectively reduce the reflection of sunlight from the surface of the silicon wafer, which can significantly increase the efficiency of solar cells [1].

There are several performance criteria for ARC. Among them are: control of the refractive index (n) of ARC, high transmittance for a wide solar spectrum, and the structure of the front surface of solar cells [2]. Various materials and thin films, including SiO<sub>2</sub>, SiN<sub>x</sub>, TiO<sub>2</sub>, Al<sub>2</sub>O<sub>3</sub>, etc., have been used for antireflective coating purposes depending on the type of solar cells [3]. Modern ARC are usually manufactured using single or multilayer thin films. An ideal antireflection structure

should lead to zero reflection loss on the solar cell surfaces over a wide solar spectral range for all incidence angles. It is well known that reflection at normal incidence at a specific wavelength (typically 600 nm) can be minimized by using a single layer with an optical thickness of a quarter wavelength. However, the materials used to deposit an antireflective layer must have a refractive index  $n=(n_{Si} \times n_0)^{1/2}$ , where  $n_0$  is the refractive index of the surrounding medium. Simple thin film antireflective coatings are limited by the availability of materials with the required refractive indices [4]. However, a single antireflective layer is also known to be unable to cover a wide range of the solar spectrum [5, 6], and the use of a double antireflective layer is being considered. The refractive indices and thickness of each of the top and bottom layers forming the antireflective stack must satisfy a number of conditions. To improve the performance of our antireflective systems, let's

study the effects of the fundamental parameters of our ARCs on the optical characteristics. First, we will perform an optimization that will look at the reflection of ARCs of different materials. The latter will allow us to see which of these materials gives us a near zero reflection for obtaining a good performance of the solar cell.

## 2. Modeling and Simulations Procedure

To design antireflective multilayers on a substrate

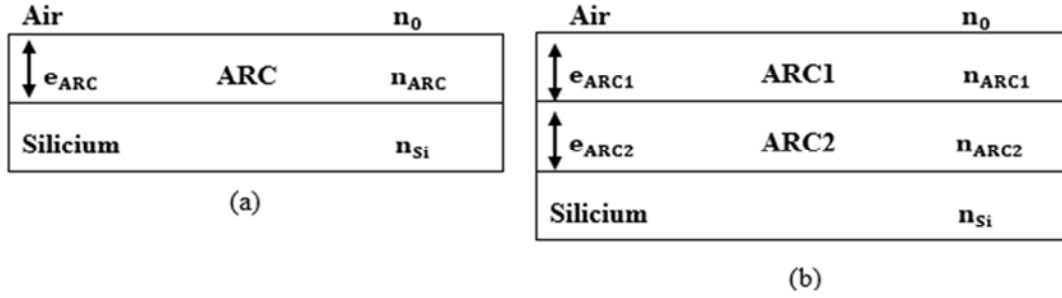


**Figure 1.** Structure of the solar cell with a single antireflection layer (a); (b) Structure of the solar cell with a double antireflection layer.

The refractive indices of the different layers must respect the following relationship:

$$n_{Si} > n_{ARC} > n_0 \quad (1)$$

$$n_{Si} > n_{ARC2} > n_{ARC1} > n_0 \quad (2)$$

First, we can describe the characteristic of a single layer matrix. This matrix concerns the tangential components of the electric field  $E$  (Z) and the magnetic fields  $H$  (Z) on the boundary layers  $Z=0$  and  $Z=Si$ .

$$\begin{pmatrix} E(0) \\ H(0) \end{pmatrix} = M \begin{pmatrix} E(Si) \\ H(Si) \end{pmatrix} \quad (3)$$

M the matrix given by:

$$\begin{pmatrix} \cos \varphi & \frac{j \cdot \sin \varphi}{n_{ARC}} \\ j \cdot n_{ARC} \cdot \sin \varphi & \cos \varphi \end{pmatrix} \quad (4)$$

The characteristic matrix of a multilayer is a product of matrices corresponding to a single layer. In the case of a double layer antireflection the relationship becomes:

$$\begin{pmatrix} E(0) \\ H(0) \end{pmatrix} = M_1 \cdot M_2 \begin{pmatrix} E(Si) \\ H(Si) \end{pmatrix} \quad (5)$$

$$\begin{pmatrix} E(0) \\ H(0) \end{pmatrix} = M_t \begin{pmatrix} E(Si) \\ H(Si) \end{pmatrix} \quad (6)$$

$$M_t = \begin{pmatrix} \cos \varphi_1 & \frac{j \cdot \sin \varphi_1}{n_{ARC1}} \\ j \cdot n_{ARC1} \cdot \sin \varphi_1 & \cos \varphi_1 \end{pmatrix} \begin{pmatrix} \cos \varphi_2 & \frac{j \cdot \sin \varphi_2}{n_{ARC2}} \\ j \cdot n_{ARC2} \cdot \sin \varphi_2 & \cos \varphi_2 \end{pmatrix} \quad (7)$$

With  $i^2 = -1$ ,  $n_{ARC1}$  and  $n_{ARC2}$  are the refractive index of the lower and upper antireflection layer, respectively.,  $\varphi_1$  and  $\varphi_2$  are respectively the phase shift between the reflected waves of layers  $i$  and  $i + 1$ .

$$\varphi_1 = \frac{2\pi\delta_1}{\lambda} \quad (8)$$

material with a refractive index  $n_s$ , we used the matrix method. The process of this method is to adjust the electric and magnetic field of the incident light on the surface of the antireflection multilayers [7]. For each configuration, a modified transfer matrix method [8-10] is used to calculate the reflectance of the silicon surface. Figure 1 shows the structures of a solar cell with a single antireflective layer (a) and a multiple antireflective layer cell (b).

$$\varphi_2 = \frac{2\pi\delta_2}{\lambda} \quad (9)$$

With  $\delta_1$  and  $\delta_2$  are the differences of steps.

$$\delta_1 = 2n_{ARC1} \cos \theta_1 \quad (10)$$

$$\delta_2 = 2n_{ARC2} \cos \theta_2 \quad (11)$$

Expressions (8) and (9) become:

$$\varphi_1 = \frac{4\pi n_{ARC1} \cos \theta_1}{\lambda} \quad (12)$$

$$\varphi_2 = \frac{4\pi n_{ARC2} \cos \theta_2}{\lambda} \quad (13)$$

A detailed derivation of the amplitude reflection coefficients  $r$  and the amplitude transmission coefficients  $t$  is given in. The resulting expressions are represented in the following equations [11]:

$$r = \frac{n_0 M_{11} + n_0 n_s M_{12} + M_{21} - n_s M_{22}}{n_0 M_{11} + n_0 n_s M_{12} + M_{21} + n_s M_{22}} \quad (14)$$

$$t = \frac{2n_0}{n_0 M_{11} + n_0 n_s M_{12} + M_{21} + n_s M_{22}} \quad (15)$$

$M_{ij}$  are the elements of the characteristic matrix of the multilayer. The energy coefficients (reflectivity, transmissivity and absorptivity) are given by:

$$R = rr^* = |r|^2 \quad (16)$$

$$T = \frac{n_{Si}}{n_0} |t|^2 \quad (17)$$

$$R + T = 1 \quad (18)$$

With  $n_{Si}$  and  $n_0$  being respectively the refractive indices of silicon and air.

### 3. Study of a Simple Antireflection Layer

The purpose of depositing a thin layer on silicon is to maximize the light transmitted to the active region of the solar cell, which in turn maximizes the current produced by the cell. If the thickness of the optical layer ( $e \times n_{Si}$ ) is equal to a quarter of the wavelength ( $\lambda$ ), the phase difference becomes  $\pi$  and the two reflected waves cancel out. For complete annihilation, the amplitude of the interfering radiation must also be the same. Under normal incidence, this requirement is met when the refractive index of the film is equal to the square root of the refractive index of the substrate [12]. Then, the optimal thickness and the optimal refractive index of the antireflective layer are given by the following relations, respectively:

$$e_{ARC} = \frac{\lambda}{4n_{ARC}} \quad (19)$$

$$n_{ARC} = \sqrt{n_0 \cdot n_{Si}} \quad (20)$$

Various materials are used as an antireflection layer. For our studies, we focused on the deposition of some materials as an antireflection layer on the solar cell and studied the efficiency of the latter. Table 1 shows the refractive indices deposited on silicon.

**Table 1.** Refractive indices of some materials.

Materials	Refractive indices at 600 nm
MgF <sub>2</sub>	1,37-1,38
SiO <sub>2</sub>	1,45-1,46
Al <sub>2</sub> O <sub>3</sub>	1,76
Si <sub>3</sub> N <sub>4</sub>	2,04
TiO <sub>2</sub>	2,20-2,40
TeO <sub>2</sub>	2,25

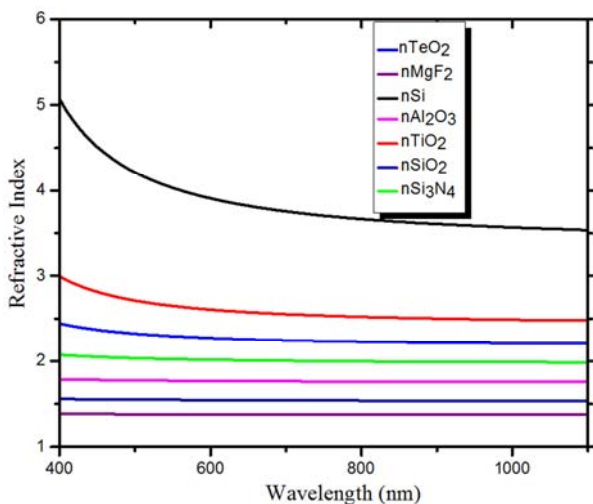


**Figure 2.** Refractive index of materials as a function of wavelength.

These refractive indices are those obtained at the reference wavelength 600 nm. To predict the behavior of the ARC for the whole illumination spectrum, it is necessary to study the evolution of these indices as a function of the wavelength (figure 2).

These materials established in the previous table, allow us

to highlight the reflection of SARC. Thus, Figure 3 represents the variation of the reflection of materials deposited as ARC as a function of the reference wavelength ( $\lambda_0=600$  nm).

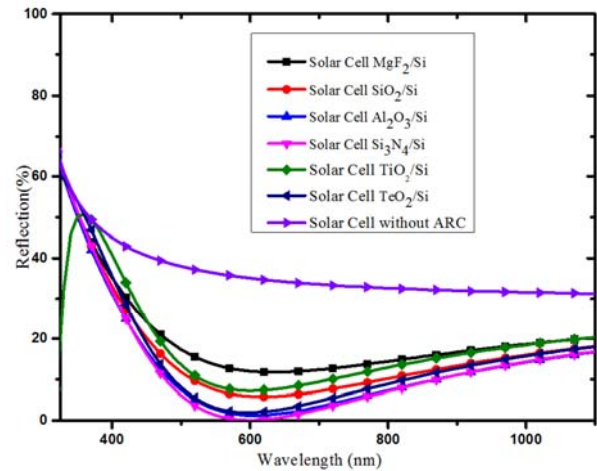


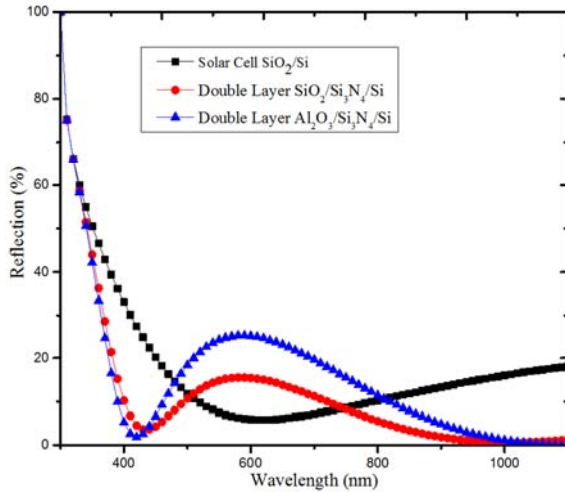
**Figure 3.** Variation of the reflection of materials deposited as ARC as a function of the reference wavelength  $\lambda_0$  ( $\lambda_0=600$  nm).

This figure represents the variation of the reflection of different materials as a function of the reference wavelength  $\lambda_0$  ( $\lambda_0=600$  nm). The use of ARC on silicon significantly reduces the reflection of the beam on the PV cell. For Si, it was noted that its reflectivity decreases sharply for wavelength ranges between 325 and 600 nm and gradually decreases for wavelengths above 600 nm. In addition, for materials used as ARC it was noted that the reflection of these materials, undergoes a considerable decrease for wavelengths between 325 and 600 nm. This is not the case for TiO<sub>2</sub> which presents a peak at 350 nm. For wavelengths above 600 nm, a slight increase in the reflection of these materials was noted. For the wavelength 600 nm, we observe a minimum and a reflection almost zero (or low); as soon as we move away from this reference wavelength, the reflection increases again. This increase is more important on the side of shorter lengths than on the side of the long wavelengths. The overall interpretation that can be drawn from these analyses and this figure is that the values of the thicknesses and refractive indices are close to the values imposed by equations (19) and (20). For example, silicon nitride (Si<sub>3</sub>N<sub>4</sub>) has a refractive index ( $n=2.04$ ) close to the refractive index of the substrate which is silicon (at  $\lambda_{ref}=600$  nm  $n_{Si}=1.963$ ). This is the reason why its reflectivity is almost zero.

### 4. Study of an Antireflective Double Layer

We know that the deposition of a SARC does not significantly reduce the optical losses. It is possible to minimize them further and for that a low-cost option would be to develop DARC. Various studies on double antireflective coatings have been reported, where different types of materials and different techniques have been

employed; however, the techniques separately require a layer developed by formalization of silicon oxide ( $\text{SiO}_2$ ) for surface passivation. The deposition of DARC must respect the fact that the refractive indices of the layers must be decreased with respect to the substrate which is silicon ( $n_{\text{Si}}=3.94$  at 650 nm (reference  $\lambda$ )) as shown in Figure 4. For example, for the DARC Air/ $\text{SiO}_2$ / $\text{Si}_3\text{N}_4$ /Si we have:  $n_{\text{Air}} < n_{\text{SiO}_2} < n_{\text{Si}}$ . Figure 4 represents the Variation of the reflection of a SARC ( $\text{SiO}_2$ /Si) and two DARC ( $\text{SiO}_2$ / $\text{Si}_3\text{N}_4$ /Si,  $\text{Al}_2\text{O}_3$ / $\text{Si}_3\text{N}_4$ /Si) as a function of the wavelength calibrated at 600 nm.



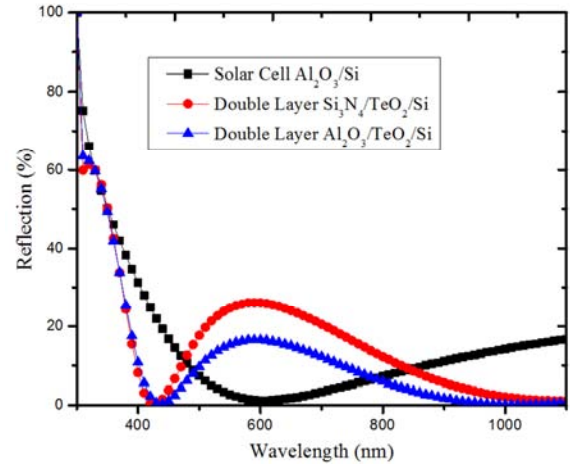
**Figure 4.** Reflection variation of one SARC ( $\text{SiO}_2$ /Si) and two DARC ( $\text{SiO}_2$ / $\text{Si}_3\text{N}_4$ /Si,  $\text{Al}_2\text{O}_3$ / $\text{Si}_3\text{N}_4$ /Si) as a function of the reference wavelength  $\lambda_0$  ( $\lambda_0=600$  nm).

Figure 4 shows that for two double layers of  $\text{SiO}_2$ / $\text{Si}_3\text{N}_4$ /Si and  $\text{Al}_2\text{O}_3$ / $\text{Si}_3\text{N}_4$ /Si, the reflection coefficient is minimal but not zero for short wavelengths and zero for long wavelengths. The explanation that can be attributed to these phenomena is that the values of the refractive index and thicknesses of these materials are optimal for long wavelengths, but it is the opposite case for short wavelengths. Moreover, this figure also shows us that for the simple antireflective coating  $\text{SiO}_2$  on silicon the reflectivity is minimal but not zero for the reference wavelength. This may be related to the fact that the values of the refractive indices of  $\text{SiO}_2$  differ from those imposed by the amplitude condition. However, these three types of ARCs ensure their role of antireflection, because their reflectivities are lower than 30%. Now, the ARC of the  $\text{SiO}_2$ /Si cell is replaced by  $\text{Al}_2\text{O}_3$  and so are the two double layers; varying the wavelength. Figure 5 shows us the evolution of the reflectivity for this ARC as well as for the two types of DARC  $\text{Si}_3\text{N}_4$ / $\text{TeO}_2$ /Si and  $\text{Al}_2\text{O}_3$ /Si.

The same phenomenon is observed in the case of the CAR  $\text{Al}_2\text{O}_3$ /Si whose reflectivity is highlighted in figure 5. The refractive index of  $\text{Al}_2\text{O}_3$  being closer to that imposed by the amplitude condition, its reflection coefficient is almost zero at the reference wavelength.

The following DARC  $\text{Si}_3\text{N}_4$ / $\text{TeO}_2$ /Si and  $\text{Al}_2\text{O}_3$ / $\text{TeO}_2$ /Si show high reflectivities compared to the  $\text{Al}_2\text{O}_3$ /Si ARC in the wavelength range 500 nm-800 nm. On the other hand, we

notice two areas of low reflectivity for wavelengths of 450 nm and 1000 nm. To consolidate our idea of verifying the impact of the refractive index of the layers on our reflectivity, let us change the  $\text{Al}_2\text{O}_3$  layer by  $\text{Si}_3\text{N}_4$  of higher refractive index (2.04). The new configuration of ARC  $\text{Si}_3\text{N}_4$ /Si shows almost zero reflectivity on the reference wavelength.



**Figure 5.** Reflection variation of one SARC ( $\text{Al}_2\text{O}_3$ /Si) and two DARC ( $\text{Si}_3\text{N}_4$ / $\text{TeO}_2$ /Si,  $\text{Al}_2\text{O}_3$ / $\text{TeO}_2$ /Si) as a function of the reference wavelength  $\lambda_0$  ( $\lambda_0=600$  nm).

Similarly, by making another configuration of DARC ( $\text{Si}_3\text{N}_4$ / $\text{TiO}_2$ /Si,  $\text{TeO}_2$ / $\text{TiO}_2$ /Si), it was noted that the following figure 6 has the same evolution as the two previous figures what differentiates them is in the variation of the reflection of DARC for long wavelengths. This is related to the fact that the difference in the refractive indices of the materials used as DARC is less important than that of the two previous cases  $\text{SiO}_2$ / $\text{Si}_3\text{N}_4$ /Si,  $\text{Al}_2\text{O}_3$ / $\text{Si}_3\text{N}_4$ /Si and  $\text{Si}_3\text{N}_4$ / $\text{TiO}_2$ /Si,  $\text{TeO}_2$ / $\text{TiO}_2$ /Si. This allows us to obtain a less photon transmission in Si compared to the two previous curves.

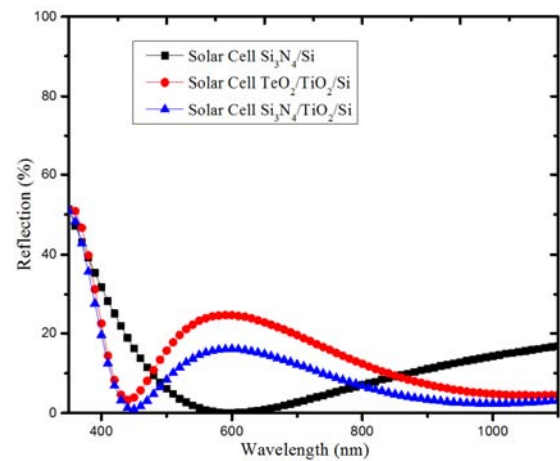


**Figure 6.** Reflection variation of one SARC ( $\text{Si}_3\text{N}_4$ /Si) and two DARC ( $\text{Si}_3\text{N}_4$ / $\text{TiO}_2$ /Si,  $\text{TeO}_2$ / $\text{TiO}_2$ /Si) as a function of the reference wavelength  $\lambda_0$  ( $\lambda_0=600$  nm).

Finally, from the results obtained in the three previous cases, we can deduce that the single anti-reflective layer is more sensitive to the reference wavelength than the double



layer. In addition, these results led us to conclude that the ARC is more interesting than the double layer around the reference wavelength.

## 5. External Quantum Efficiency of a Solar Cell

The solar cell used to evaluate the spectral response with and without ARC, is an ideal p – n junction whose parameters have the following values:

- 1) Silicon cellulose transmitter thickness: 0.5  $\mu\text{m}$ ;
- 2) Total thickness of silicon cellulose: 200  $\mu\text{m}$ ;
- 3) Transmitter doping (p-zone):  $N_d=10^{19} \text{ cm}^{-3}$ ;
- 4) Base Doping (Zone n):  $N_a=10^{16} \text{ cm}^{-3}$
- 5) Recombination speed on the front face  $S_p=0 \text{ cm.s}^{-1}$
- 6) Recombination speed at rear surface  $S_n=0 \text{ cm.s}^{-1}$  (BSF).

Figure 7 shows the external quantum efficiency or spectral response of the cell without ARC and then with 3 distinct ARC as a function of the calibrated wavelength at 600 nm.

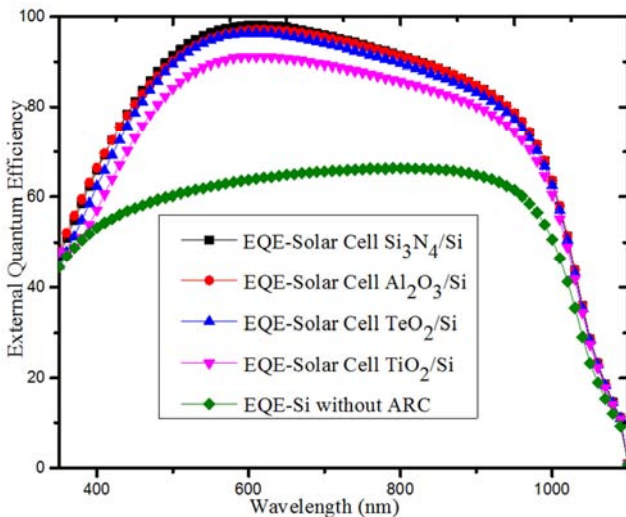


**Figure 7.** External quantum efficiency of cells with and without ARC as a function of reference wavelength  $\lambda_0$  ( $\lambda_0=600 \text{ nm}$ ).

This figure shows that for wavelength ranges between 350 and 600 nm, it found a rapid increase in the quantum efficiency of the materials and for wavelengths above 600 nm a progressive decrease in the external quantum efficiency was noted. While without antireflection layer and with a strong reflection on the surface of the emitter, the external quantum efficiency does not exceed 65%. Moreover, it found that among the used material configurations the external quantum efficiency of the  $\text{Si}_3\text{N}_4/\text{Si}$  configuration is the best compared to the others. The fact is that for low wavelengths, it has noted a strong presence of energy of the materials which is higher than the gap energy of silicon causing a decrease of the reflection. This decrease in reflection is synonymous with a strong transmission and a strong absorption generating an important generation of charge carriers causing the increase of the external quantum efficiency of the cell. For long wavelengths, it has found a lower energy of the material which is lower than the gap

energy of silicon resulting in a strong reflection, that is to say a low transmission and absorption. Finally, the explanation that we can attribute to the importance of the external quantum yield of the  $\text{Si}_3\text{N}_4/\text{Si}$  configuration compared to the others is that the refractive index of  $\text{Si}_3\text{N}_4$  ( $n=2.04$ ) is close to the optimal index ( $\sqrt{n_{\text{air}} \times n_{\text{Si}}}$ ) coming from the magnitude condition.

After we run simulations and get results on the external quantum efficiency of the ARC, we will do the same for the DARC. In these simulations,  $\text{TiO}_2$ , which has a large refractive index, was fixed and associated with materials with a smaller refractive index. Figure 8 shows the external quantum efficiency or spectral response of cells with and without DARC as a function of the calibrated wavelength at 600 nm.

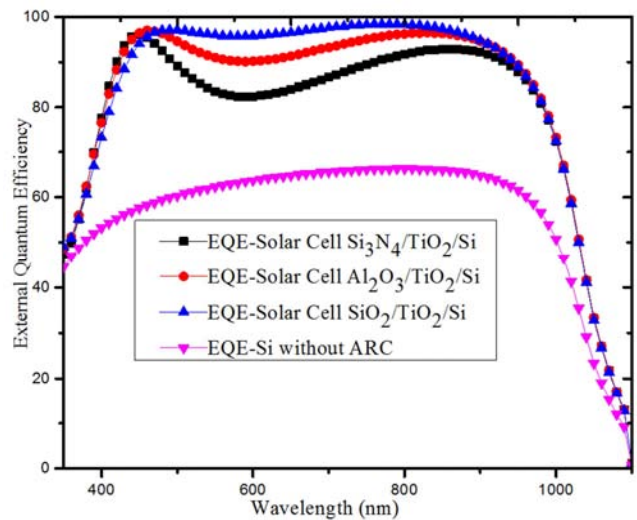


**Figure 8.** External quantum efficiency of cells with and without DCAR as a function of reference wavelength  $\lambda_0$  ( $\lambda_0=600 \text{ nm}$ ).

In this figure, it has highlighted the external quantum efficiency of the different DARC configurations as a function of the wavelength. For wavelength ranges between 350 and 450 nm, it's noticed that the external quantum efficiency of the DARC configurations is important approaching 98%. Then, it's noted a decrease in the external quantum yield between 450 and 800 nm, but this is slight for the  $\text{SiO}_2/\text{TiO}_2/\text{Si}$  configuration. Finally, it's noted again that the external quantum efficiency increases between 800 and 900 nm before decreasing for wavelengths above 900 nm. The interpretation that it can draw is that for low wavelengths, it's observed a strong absorption in the vicinity of the sea surface which justifies the strong increase of the quantum efficiency for wavelength ranges between 350 and 450 nm. This phenomenon is observed at the second peak, i.e. for wavelengths between 800 and 900 nm (close to the infrared). Moreover, it should be understood that the configurations of two layers of refractive index with an excellent gap allow us to widen the spectral band with a significant external quantum efficiency.

## 6. Conclusion

In this paper, a theoretical study of the optical properties of

antireflective coatings has been made. By presenting some materials generally used as antireflection, their optical properties, such as reflection and transmission, have been studied. Therefore, the influence of their thicknesses on these optical constants has been highlighted, by the fact that it can participate in the improvement of the transmission of the luminous flux in the substrate on which this layer is deposited. Among these materials used; silicon dioxide ( $\text{SiO}_2$ ), sapphire ( $\text{Al}_2\text{O}_3$ ), silicon nitride ( $\text{Si}_3\text{N}_4$ ), and tellurium dioxide ( $\text{TeO}_2$ ) have shown interesting properties because reducing to less than 10% the reflectivity. In addition, the reflectivity of these materials becomes practically zero if and only if the refractive index of the latter is close to the optimal index. For the reflectivity to be zero, it is necessary that a reference wavelength which is equal to 600 nm in our work. However, by making a combination of a double layer of these materials, we noticed that these reduce the optical losses better than the single layer. But also the studies on the spectral response of these materials allowed us to understand that the gap between the combinations of these materials plays a role in obtaining a good efficiency of the cell.

## References

- [1] Q. Ma, W. J. Zhiang, D. H. Ma, Z. Q. Fan, X. B. Ma, "Optimal design of quadruple-layer antireflection coating structure for conversion efficiency enhancement in crystalline silicon solar cells", *International Journal for Light and Electron Optics* (2010), doi.org/10.1016/j.ijleo.2017.12.024, pp. 1-12.
- [2] S. Sali, S. Kermadi, L. Zougar, B. Benzaoui, N. Saoula, K. Mahdid, F. Aitameur, M. Boumaour, "Nanocrystalline properties of  $\text{TiO}_2$  thin film deposited by ultrasonic spray pulverization as an anti-reflection coating for solar cells applications", *Journal of ELECTRICAL ENGINEERING*, VOL 68 (2017), NO 7, pp. 24-30.
- [3] H. Kanda, A. Uzum, N. Harano, S. Yoshinaga, Y. Ishikawa, Y. Uraoka, H. Fukui, T. Harado, S. Ito, " $\text{Al}_2\text{O}_3/\text{TiO}_2$  double layer anti-reflection coating film for crystalline silicon solar cells formed by spray pyrolysis", *Energy Science and Engineering* 2016; 4 (4): pp. 269-276.
- [4] M. M. Diop, A. Diaw, N. Mbengue, O. Ba, M. Diagne, O. A. Niasse, B. Ba, J. Sarr, "Optimization and Modeling of Antireflective Layers for Silicon Solar Cells: In Search of Optimal Materials", *Materials Sciences and Applications*, 9, 705-722.
- [5] Strehlke, S., Bastide, S., Guillet, J. and Lévy-Clément, C. (2011) Design of Porous Silicon Antireflection Coatings for Silicon Solar Cells. *Materials Science and Engineering*, 69, 81-86.
- [6] Lee, I., Lim, D. G., Lee, S. H. and Yi, J. (2001) The Effect of a Double Layer An-ti-Reflection Coating for a Buried Contact Solar Cell Application. *Surface and Coatings Technology*, 137, 86-91. [https://doi.org/10.1016/S0257-8972\(00\)01076-8](https://doi.org/10.1016/S0257-8972(00)01076-8).
- [7] Md. S. Sarker, M. F. Khatun, S. R. A. Ahmed, J. Hossain, "Optimization of multilayer antireflection coatings for improving performance of silicon solar cells", *International Conference on Computer, Communication, Chemical, Materials and Electronic Engineering (IC4ME2)*, 11-12 July, 2019.
- [8] Katsidis, C. C. and Siapakas, D. I. (2002) General Transfer-Matrix Method for Optical Multilayer Systems with Coherent, Partially Coherent, and Incoherent Interference. *Applied Optics*, 41, 3978-3987. <https://doi.org/10.1364/AO.41.003978>.
- [9] Troparevsky, M. C., Sabau, A. S., Lupini, A. R. and Zhang, Z. (2010) Transfer-Matrix Formalism for the Calculation of Optical Response in Multilayer Systems: From Coherent to Incoherent Interference. *Optics Express*, 18, 24715-24721.
- [10] Sahoo, K. C., Lin, M.-K., Chang, E.-Y., Lu, Y.-Y., Chen, C.-C., Huang, J.-H. and Chang, C.-W. (2009) Fabrication of Antireflective Sub-Wavelength Structures on Silicon Nitride Using Nano Cluster Mask for Solar Cell Application. *Nanoscale Re-search Letters*, 4, 680-683. <https://doi.org/10.1007/s11671-009-9297-7>.
- [11] A. Diaw, N. Mbengue, M. M. Diop, O. Ba, F. I Barro, B. Ba, "Modeling and Simulation of Antireflecting layers, influencing parameters on the Reflexion and Transmission on the Silicon Solar Cells.", *Physics and Materials Chemistry*. 2015, 3 (3), 37-39 DOI: 10.12691/pmc-3-3-1.
- [12] M. Victoria, C. Domínguez, I. Antón, G. Sala, "Antireflective coatings for multijunction solarcells under wide-angle ray bundles", *Optical Society of America*, Vol. 20, No. 7, pp. 8136-8147.